

SELECTED RESEARCH ABSTRACTS 2010-2011

UPMC Eye Center
Department of Ophthalmology

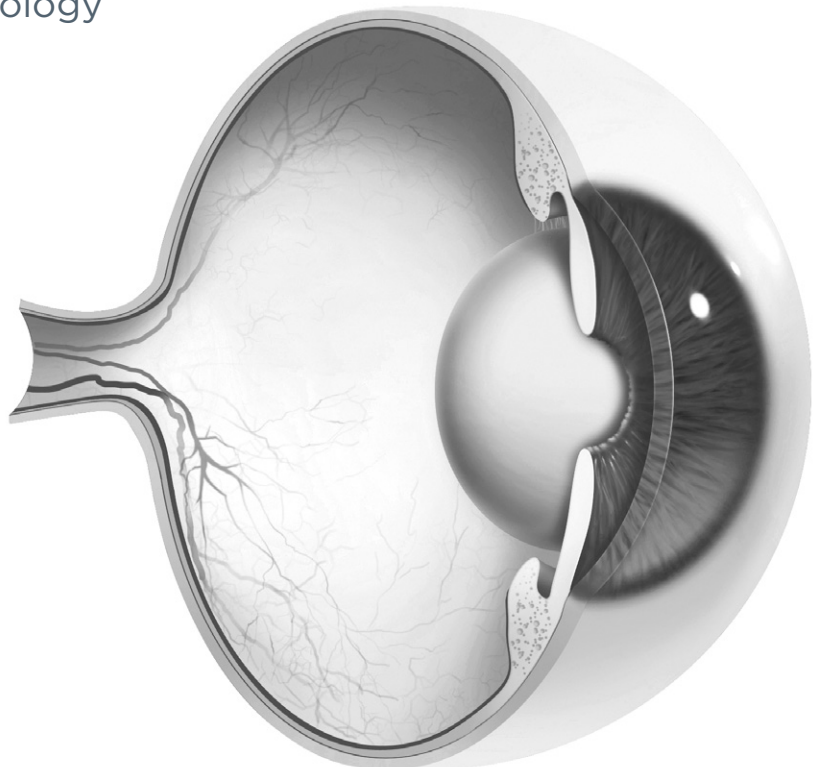


TABLE OF CONTENTS

SELECTED 2010-2011 ABSTRACTS

Identification and assessment of Schlemm's canal by spectral-domain optical coherence tomography	3
Kagemann L, Wollstein G, Ishikawa H, Bilonick RA, Brennen PM, Folio LS, Gabriele ML, Schuman JS.	
Adipose-derived stem cells differentiate to keratocytes in vitro	4
Du Y, Roh DS, Funderburgh ML, Mann MM, Marra KG, Rubin JP, Li X, Funderburgh JL.	
Three dimensional optical coherence tomography imaging: advantages and advances	5
Gabriele ML, Wollstein G, Ishikawa H, Xu J, Kim J, Kagemann L, Folio LS, Schuman JS.	
Kruppel-like factors: three fingers in control	5
Swamynathan SK.	
AzaSite® inhibits Staphylococcus aureus and coagulase-negative	6
Staphylococcus biofilm formation in vitro	
Wu EC, Kowalski RP, Romanowski EG, Mah FS, Gordon YJ, Shanks RM.	
Responses of cultured human keratocytes and myofibroblasts to ethyl pyruvate: a microarray analysis of gene expression	7
Harvey SA, Guerriero E, Charukamnoetkanok N, Piluek J, Schuman JS, Sundarraj N.	
Delaying the expression of herpes simplex virus type 1 glycoprotein B (gB) to a true late gene alters neurovirulence and inhibits the gB-CD8+ T-cell response in the trigeminal ganglion	8
Ramachandran S, Davoli KA, Yee MB, Hendricks RL, Kinchington PR.	

Identification and assessment of Schlemm's canal by spectral-domain optical coherence tomography

Author: Kagemann L, Wollstein G, Ishikawa H, Bilonick RA, Brennen PM, Folio LS, Gabriele ML, Schuman JS.

Journal: *Invest Ophthalmol Vis Sci* 2010 August;51(8):4054-4059.

PURPOSE:

Measurements of human Schlemm's canal (SC) have been limited to histologic sections. The purpose of this study was to demonstrate noninvasive measurements of aqueous outflow (AO) structures in the human eye, examining regional variation in cross-sectional SC areas (on/off collector channel [CC] ostia [SC/CC] and nasal/temporal) in the eyes of living humans.

METHODS:

SC was imaged by spectral-domain optical coherence tomography with a 200-nm bandwidth light source. Both eyes of 21 healthy subjects and one glaucomatous eye of three subjects were imaged nasally and temporally. Contrast and magnification were adjusted to maximize visualization. Cross-sectional SC on and off SC/CC was traced three times by two independent masked observers using ImageJ (ImageJ 1.40g, <http://rsb.info.nih.gov/ij/> Wayne Rasband, developer, National Institutes of Health, Bethesda, MD). The mean SC area was recorded. A linear mixed-effects model was used to analyze eye, nasal/temporal laterality, and SC area on or off SC/CC.

RESULTS:

SC area was significantly larger on SC/CCs than off (12,890 vs. 7,391 microm², P < 0.0001) and was significantly larger on the nasal side than on the temporal (10,983 vs. 8,308 microm², P = 0.009). SC areas were significantly smaller in glaucoma patients than in normal subjects, whether pooled (P = 0.0073) or grouped by on (P = 0.0215) or off (P = 0.0114) SC/CC.

CONCLUSIONS:

Aqueous outflow structures, including SC and CCs, can be noninvasively assessed in the human eye. These measurements will be useful in physiological studies of AO and will be clinically useful in the determination of the impact of glaucoma therapies on IOP as well as presurgical planning.

For the full list of abstracts, please visit
UPMCPhysicianResources.com/abstracts.



Adipose-derived stem cells differentiate to keratocytes in vitro

Author: Du Y, Roh DS, Funderburgh ML, Mann MM, Marra KG, Rubin JP, Li X, Funderburgh JL.

Journal: Mol Vis 2010;16:2680-2689.

PURPOSE:

Adipose-derived stem cells (ADSC) are an abundant population of adult stem cells with the potential to differentiate into several specialized tissue types, including neural and neural crest-derived cells. This study sought to determine if ADSC express keratocyte-specific phenotypic markers when cultured under conditions inducing differentiation of corneal stromal stem cells to keratocytes.

METHODS:

Human subcutaneous adipose tissue was obtained by lipoaspiration. ADSC were isolated by collagenase digestion and differential centrifugation. Side population cells in ADSC were demonstrated using fluorescence-activated cell sorting after staining with Hoechst 33342. Differentiation to keratocyte phenotype was induced in fibrin gels or as pellet cultures with serum-free or reduced-serum media containing ascorbate. Keratocyte-specific gene expression was characterized using western blotting, quantitative RT-PCR, and immunostaining.

RESULTS:

ADSC contained a side population and exhibited differentiation to adipocytes and chondrocytes indicating adult stem-cell potential. Culture of ADSC in fibrin gels or as pellets in reduced-serum medium with ascorbate and insulin induced expression of keratan, keratan sulfate, and aldehyde dehydrogenase 3 family, member A1 (ALDH3A1), products highly expressed by differentiated keratocytes. Expression of differentiation markers was quantitatively similar to corneal stromal stem cells and occurred in both serum-free and serum containing media.

CONCLUSIONS:

ADSC cultured under keratocyte-differentiation conditions express corneal-specific matrix components. Expression of these unique keratocyte products suggests that ADSC can adopt a keratocyte phenotype and therefore have potential for use in corneal cell therapy and tissue engineering.

For the full list of abstracts, please visit
UPMCPhysicianResources.com/abstracts.



Three dimensional optical coherence tomography imaging: advantages and advances

Author: Gabriele ML, Wollstein G, Ishikawa H, Xu J, Kim J, Kagemann L, Folio LS, Schuman JS.

Journal: Prog Retin Eye Res 2010 November;29(6):556-579.

ABSTRACT:

Three dimensional (3D) ophthalmic imaging using optical coherence tomography (OCT) has revolutionized assessment of the eye, the retina in particular. Recent technological improvements have made the acquisition of 3D-OCT datasets feasible. However, while volumetric data can improve disease diagnosis and follow-up, novel image analysis techniques are now necessary in order to process the dense 3D-OCT dataset. Fundamental software improvements include methods for correcting subject eye motion, segmenting structures or volumes of interest, extracting relevant data post hoc and signal averaging to improve delineation of retinal layers. In addition, innovative methods for image display, such as C-mode sectioning, provide a unique viewing perspective and may improve interpretation of OCT images of pathologic structures. While all of these methods are being developed, most remain in an immature state. This review describes the current status of 3D-OCT scanning and interpretation, and discusses the need for standardization of clinical protocols as well as the potential benefits of 3D-OCT scanning that could come when software methods for fully exploiting these rich datasets are available clinically. The implications of new image analysis approaches include improved reproducibility of measurements garnered from 3D-OCT, which may then help improve disease discrimination and progression detection. In addition, 3D-OCT offers the potential for preoperative surgical planning and intraoperative surgical guidance.

Kruppel-like factors: three fingers in control

Author: Swamynathan SK.

Journal: Hum Genomics 2010 April;4(4):263-270.

ABSTRACT:

Kruppel-like factors (KLFs), members of the zinc-finger family of transcription factors capable of binding GC-rich sequences, have emerged as critical regulators of important functions all over the body. They are characterised by a highly conserved C-terminal DNA-binding motif containing three C2H2 zinc-finger domains, with variable N-terminal regulatory domains. Currently, there are 17 KLFs annotated in the human genome. In spite of their structural similarity to one another, the genes encoding different KLFs are scattered all over the genome. By virtue of their ability to activate and/or repress the expression of a large number of genes, KLFs regulate a diverse array of developmental events and cellular processes, such as erythropoiesis, cardiac remodelling, adipogenesis, maintenance of stem cells, epithelial barrier formation, control of cell proliferation and neoplasia, flow-mediated endothelial gene expression, skeletal and smooth muscle development, gluconeogenesis, monocyte activation, intestinal and conjunctival goblet cell development, retinal neuronal regeneration and neonatal lung development. Characteristic features, nomenclature, evolution and functional diversities of the human KLFs are reviewed here.

AzaSite® inhibits *Staphylococcus aureus* and coagulase-negative *Staphylococcus* biofilm formation in vitro

Author: Wu EC, Kowalski RP, Romanowski EG, Mah FS, Gordon YJ, Shanks RM.

Journal: *J Ocul Pharmacol Ther* 2010 December;26(6):557-562.

PURPOSE:

The aim of this study was to analyze the effect of azithromycin (AZM) 1% ophthalmic solution in DuraSite® (AzaSite®) on biofilm formation by *Staphylococcus aureus* and coagulase-negative staphylococci in vitro.

METHODS:

Susceptible and resistant clinical strains ($n = 8$) of *S. aureus* and coagulase-negative staphylococci were challenged with serial dilutions of AzaSite and its components: AZM, benzalkonium chloride (BAK), and the DuraSite drug delivery vehicle. After 20 h of incubation, bacterial growth was quantified using a spectrophotometer ($A = 600$ nm). Plates were stained with crystal violet and biofilm formation was quantified spectrophotometrically at $A = 590$ nm.

RESULTS:

AzaSite and AZM inhibited bacterial growth ($P < 0.05$) and biofilm formation ($P < 0.05$) in AZM-susceptible strains at all studied dilutions. AZM-resistant strains treated with AzaSite exhibited a significant reduction in biofilm formation ($P < 0.05$) at subinhibitory concentrations (1.25%-5%). AZM had no effect on bacterial growth in resistant strains but conferred a small reduction in biofilm formation at concentrations from 1.25 to 10 mg/mL in most strains. DuraSite inhibited biofilm formation at concentrations between 10% and 2.5% in all studied strains ($P < 0.05$), without affecting bacterial growth. BAK inhibited bacterial growth and biofilm formation in all strains between concentrations of 0.042 and 0.375 mg/mL ($P < 0.05$).

CONCLUSIONS:

AzaSite, AZM, or BAK prevented biofilm formation by inhibiting growth of AZM-susceptible strains. AzaSite, AZM, and DuraSite also reduced biofilm formation at subinhibitory concentrations for growth. Our data indicate that AZM has a moderate inhibitory effect on biofilm formation, whereas DuraSite appears to play a greater role in the inhibition of staphylococcal biofilm formation by AzaSite.

Responses of cultured human keratocytes and myofibroblasts to ethyl pyruvate: a microarray analysis of gene expression

Author: Harvey SA, Guerriero E, Charukamnoetkanok N, Piluek J, Schuman JS, Sundarraj N.

Journal: *Invest Ophthalmol Vis Sci* 2010 June;51(6):2917-2927.

PURPOSE:

Ethyl pyruvate (EP) has pharmacologic effects that remediate cellular stress. In the organ-cultured murine lens, EP ameliorates oxidative stress, and in a rat cataract model, it attenuates cataract formation. However, corneal responses to EP have not been elucidated. In this study, the potential of EP as a therapeutic agent in corneal wound healing was determined by examining its effects on the transition of quiescent corneal stromal keratocytes into contractile myofibroblasts.

METHODS:

Three independent preparations of cultured human keratocytes were treated with TGF-beta1, to elicit a phenotypic transition to myofibroblasts in the presence or absence of 10 or 15 mM EP. Gene expression profiles of the 12 samples (keratocytes +/- EP +/- TGF-beta1 for three preparations) were produced by using gene microarrays.

RESULTS:

TGF-beta1-driven twofold changes in at least two of three experiments defined a group of 1961 genes. Genes showing twofold modulation by EP in at least two experiments appeared exclusively in myofibroblasts (857 genes), exclusively in keratocytes (409 genes), or in both phenotypes (252 genes). Analysis of these three EP-modulated groups showed that EP (1) inhibited myofibroblast proliferation with concomitant modulation of some cell cycle genes, (2) augmented the NRF2-mediated antioxidant response in both keratocytes and myofibroblasts, and (3) modified the TGF-beta1-driven transition of keratocytes to myofibroblasts by inhibiting the upregulation of a subset of profibrotic genes.

CONCLUSIONS:

These EP-induced phenotypic changes in myofibroblasts indicate the potential of EP as a therapeutic agent in corneal wound healing.

For the full list of abstracts, please visit
UPMCPhysicianResources.com/abstracts.



Delaying the expression of herpes simplex virus type 1 glycoprotein B (gB) to a true late gene alters neurovirulence and inhibits the gB-CD8+ T-cell response in the trigeminal ganglion

Author: Ramachandran S, Davoli KA, Yee MB, Hendricks RL, Kinchington PR.

Journal: *J Virol* 2010 September;84(17):8811-8820.

ABSTRACT:

Following herpes simplex virus type 1 (HSV-1) ocular infection of C57BL/6 mice, activated CD8(+) T cells specific for an immunodominant epitope on HSV-1 glycoprotein B (gB-CD8 cells) establish a stable memory population in HSV-1 latently infected trigeminal ganglia (TG), whereas non-HSV-specific CD8(+) T cells are lost over time. The retention and activation of gB-CD8 cells appear to be influenced by persistent viral antigenic exposure within the latently infected TG. We hypothesized that the low-level expression of gB from its native promoter before viral DNA synthesis is critical for the retention and activation of gB-CD8 cells in the TG during HSV-1 latency and for their ability to block HSV-1 reactivation from latency. To test this, we created a recombinant HSV-1 in which gB is expressed only after viral DNA synthesis from the true late gC promoter (gCp-gB). Despite minor growth differences compared to its rescuant in infected corneas, gCp-gB was significantly growth impaired in the TG and produced a reduced latent genome load. The gCp-gB- and rescuant-infected mice mounted similar gB-CD8 effector responses, but the size and activation phenotypes of the memory gB-CD8 cells were diminished in gCp-gB latently infected TG, suggesting that the stimulation of gB-CD8 cells requires gB expression before viral DNA synthesis. Surprisingly, late gB expression did not compromise the capacity of gB-CD8 cells to inhibit HSV-1 reactivation from latency in ex vivo TG cultures, suggesting that gB-CD8 cells can block HSV-1 reactivation at a very late stage in the viral life cycle. These data have implications for designing better immunogens for vaccines to prevent HSV-1 reactivation.



UPMC EYE CENTER

Eye & Ear Institute

203 Lothrop St.
Pittsburgh, PA 15213

UPMC.com/EyeCenter

UPMC is an equal opportunity employer. UPMC policy prohibits discrimination or harassment on the basis of race, color, religion, ancestry, national origin, age, sex, genetics, sexual orientation, marital status, familial status, disability, veteran status, or any other legally protected group status. Further, UPMC will continue to support and promote equal employment opportunity, human dignity, and racial, ethnic, and cultural diversity. This policy applies to admissions, employment, and access to and treatment in UPMC programs and activities. This commitment is made by UPMC in accordance with federal, state, and/or local laws and regulations.